Imbibition of Picoliter Water Droplets on Coated Inkjet Papers

Asaf Oko[1], Agne Swerin[1], and Per M. Claesson[1,2]*

[1] YKI, Ytkemiska Institutet AB/Institute for Surface Chemistry, Box 5607, SE-114 86 Stockholm, Sweden

[2]Department of Chemistry, Surface and Corrosion Science, Royal Institute of Technology, SE-100 44 Stockholm, Sweden

**Corresponding author. Tel.: +46 10 516 6031; fax: +46 8 208998. E-mail address: agne.swerin@yki.se (A. Swerin)*

Abstract

When an impinged inkjet droplet is impacting a paper substrate, it evaporates to the air and penetrates into the paper. The imbibition dynamics are strongly dependant on the pore structure on the surface and inside the substrate. In this work picoliter (pL) water droplets were impinged onto two commercially available matte and gloss coated paper sample. The imbibition process was recorded and analyzed using a high speed imaging system. Calculations of the volume change were done by considering that the droplets are shaped as hemispherical caps. The total drying time of water droplets of about 60 pL is 10-15 ms on the gloss coated paper, and 30-150 ms on the matte coated paper. In addition, the two samples show different regimes in the imbibition process caused by the different porous structures present in the samples.

Introduction:

Dynamics of liquid imbibition is of special interest due to its industrial applications in e.g. printing processes, and it also offers substantial fundamental research challenges. It is well established that the drying time of liquid droplets on a permeable substrate is set by the liquid evaporation rate and the imbibition rate, and that the relative importance of these processes strongly depends on the substrate characters such as porosity and surface energy as well as on the degree of liquid volatility. When a liquid droplet is impinged onto a paper coated with a porous layer it experiences evaporation, expansion of the droplet base diameter and imbibition into the porous matrix, as illustrated in Figure 1.

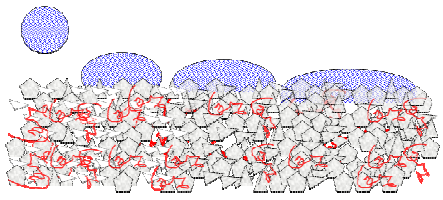

Figure 1. Illustration (not to scale) of spreading and imbibition of a liquid droplet *impinged on a paper coated with a porous layer consisting of pigment particles of different shapes and a binder (red lines).*

The Lucas Washburn[1] equation is often used to describe the capillary rise in porous networks. In the equation the height h of a liquid meniscus in a cylindrical capillary with a radius R is given by:

$$h^2 = t\frac{2\sigma R\cos\theta}{2\mu} \quad (1)$$

Where t is time, σ the liquid vapor surface tension, θ the contact angle and μ is the liquid viscosity. The capillary rise described by Eq. 1 is dominated by the viscous force exerted by the rising liquid, and the Laplace pressure exerted by the curvature of the liquid meniscus. Other equations exist in the literature describing regimes dominated by other forces[2], but the discussion of their applicability is outside the frame of this work.

From the very first moment of the impact between the droplet and the surface, both imbibition and expansion occur simultaneously. While expanding, additional surface area is engaged in the imbibition process. It is therefore useful to normalize the droplet volume by the droplet base surface area, giving an average length per surface area or *effective length* h_{eff} [3] defined as (see appendix for discussion):

$$h_{eff}(t) = C + \frac{V_0 - V(t)}{\pi R_d^2(t)} \quad (2)$$

Where C and V_0 are correction terms, $V(t)$ the droplet volume at time t, and $R_d(t)$ the sessile drop base radius at time t. When imbibition takes place h_{eff} is related to the average distance between the surface and the advancing liquid front inside the porous network, although the latter will not be equal to h_{eff} since Eq. 2 is not taking into account the porosity of the medium, tortuosity of the liquid path inside the porous medium and imbibition taking place parallel to the surface (wicking)[4].

Materials and Methods:

Two types of commercially available paper samples were used, i.e. matte coated (230 g/m^2, photo supreme double-sided matte, Staples) and gloss coated (240 g/m^2, photo plus gloss, Staples).

Liquid imbibition measurements were made using a DataPhysics OCA40 micro (DataPhysics GmbH, Germany) capable of delivering droplets with volumes in the tens of picoliter (pL) range. The system includes a high-speed CCD camera (max. 2,200 images/s) with 50x magnification, a piezoelectric dispenser (Microdrop GmbH, Germany) that delivers single 60 pL water droplets with a speed of 1.5 m/s, and a Peltier sample stage for

accurate control of the temperature. In all experiments the temperature and relative humidity were kept constant at 23±1°C, and 45 ± 3% respectively. In the analysis, a solid liquid baseline is set manually for each recorded sequence and then the analysis is done automatically by the SCA 20 software. For the volume calculation it is assumed that the droplets take the shape of a hemispherical cap.

Images of the surfaces in air were recorded using an Atomic Force Microscope (combined confocal Raman microscope/AFM/SNOM alpha300 RAS, WITec) in tapping mode using non-contact cantilevers with a spring constant of 42 N/m.

XPS measurements were carried out by using a Kratos AXIS Ultra^{DLD} X-ray photoelectron spectrometer (Kratos Analytical, Manchester, UK). The samples were analyzed using a monochromatic Al X-ray source operated at 150W (10 mA/15 kV). The analysis area was below about 1 mm^2 (with most of the signal from an area of 700 x 300 µm). In the analysis, low resolution wide spectra (pass energy 160 eV) was used to quantify the relative amounts of elements.

Scanning Electron microscopy (SEM) images were taken using JEOL JSM-7000 and JEOL JSM-7401F, in a low landing energy (0.8-1.3 keV, in gentle-beam mode). The sample area in the images was not metal coated.

Results

Each experiment is recorded, resulting in a sequence of images. Two typical image sequences are illustrated in Figure 2 and Figure 3.

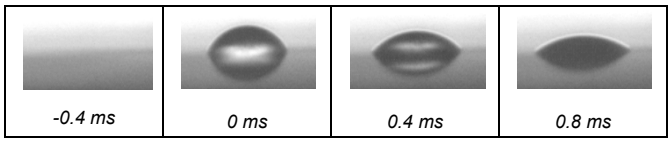

Figure 2. *A sequence of images showing a droplet impinged on a gloss coated paper. The observed droplet volume at t=0 ms was 49 pL.*

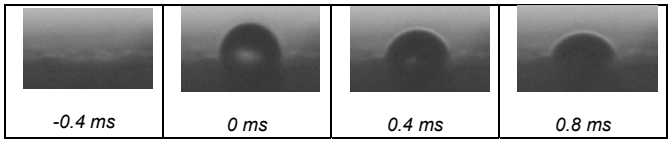

Figure 3. *A sequence of images showing a droplet impinged on a matte coated paper. The observed droplet volume at t=0 ms was 41 pL.*

The chemical composition of the gloss coated paper surface measured by XPS (Table 1) reveals a surface enriched in Alumina pigments and binder (most probably poly(vinyl alcohol) or gelatin). The surface roughness (Figure 4) exhibits rms 70 nm and peak to peak value of 550 nm (Table 1), and the baseline is well defined as seen from Figure 2.

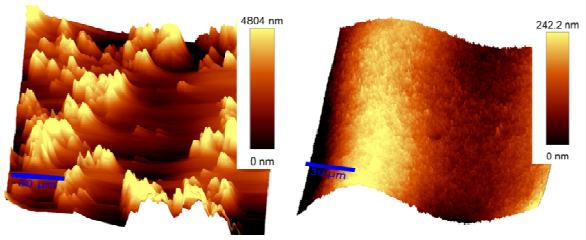

Figure 4*. AFM images. Left: Matte coated papre. RMS roughness= 1400 nm. Right: Gloss coated paper. RMS roughness=74 nm.*

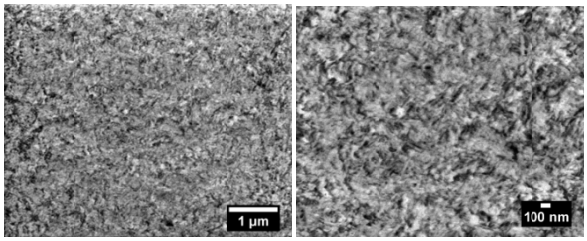

Figure 5. *SEM images of the gloss coated paper. Pore diameter range is estimated to be under 100 nm. Mind the difference in scale bar.*

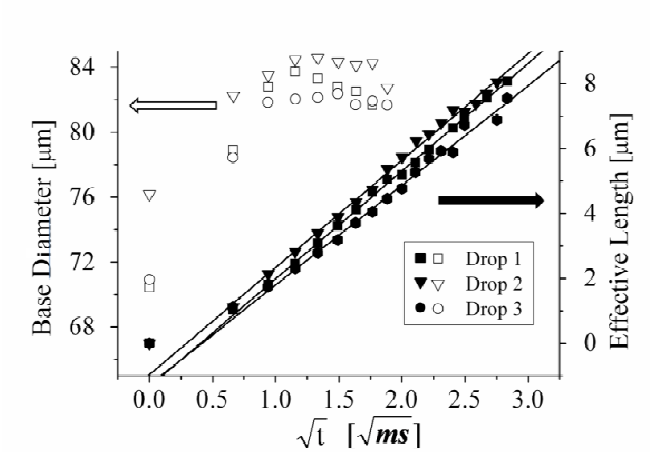

Figure 6. *Effective length (filled symbols) and base diameter (unfilled symbols) in micrometers (µm) vs. $\sqrt{t}$ ($\sqrt{ms}$) for three separate droplets impinged on gloss coated paper. The black lines are linear fits to the data.*

The gloss coated paper porous surface is visualized by SEM in Figure 5. The exact pore size and distribution cannot be determined but the range of pore diameter can be estimated to be below 100 nm. In Figure 6 the effective length and the droplet base diameter of three droplets impinged on different spots are plotted against the square root of time, together with linear curves fitted to the effective length data. In the fitting process the first three experimental points in each droplet sequence are excluded. For all three droplets, the points at 0 ms and to some extent the ones at 0.4 ms diverge from the fitted curves. The total observed drying time is similar for all droplets and measured to be 13-16 ms. The initial spreading period (defined as the time during which the base diameter reaches its maximum value) in all samples is lasting about 1.2 ms after initial paper-droplet contact.

Table 1: *Surface topography done by AFM and chemical composition done by XPS.*

Paper sample	Roughness		Surface chemical composition in atomic percentage [%]			
	RMS [nm]	, Peak to Peak [nm]	O	C	Al	Si
Gloss coated	74	550	58	16	25.0	-
Matte coated	1400	13,000	39	42	-	14.0

The chemical composition of the matte coated paper surface determined by XPS (Table 1) reveals a significant content of silicone atoms in the surface layer due to enrichment of silica gel aggregates in the coating layer. This sample exhibits a rough surface with rms roughness of 1400 nm and peak to peak value of 13,000 nm (Table 1, Figure 4 and Figure 7).

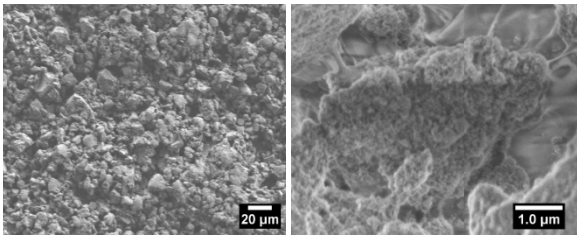

Figure 7*. SEM images of the matte coated paper. Two distinct pore populations are seen: inter and intra-aggregate (see text for discussion). Mind the difference in scale bar.*

SEM images of the matte coated paper (Figure 7) reveal two distinct pore populations: inter-aggregate and intra-aggregate. The inter-aggregate pores occur as a consequence of the gaps between the silica gel aggregates (Figure 7 left), while the intra-aggregate pores are voids inside the aggregates themselves (Figure 7 right). The difference in pore size between the two distinct pore populations is estimated to be two orders of magnitude. The time evolutions of the droplet base diameter and the effective length on the matte coated paper are shown in Figure 8. No linear fitting is done in this case, but a trend is seen in all droplets where the linear coefficient describing the rate of change in the effective length decreases after about 1.8-2.2 ms (Figure 8, inset) and at an effective length of 6-11µm. Total drying times observed on this sample are between 30-100 ms, which is a significantly larger time and larger variation than observed on the gloss coated paper (10-13 ms). The droplet initial spreading period (as defined above) is similar to the one on the gloss coated paper, lasting about 1.2 ms (Figure 8).

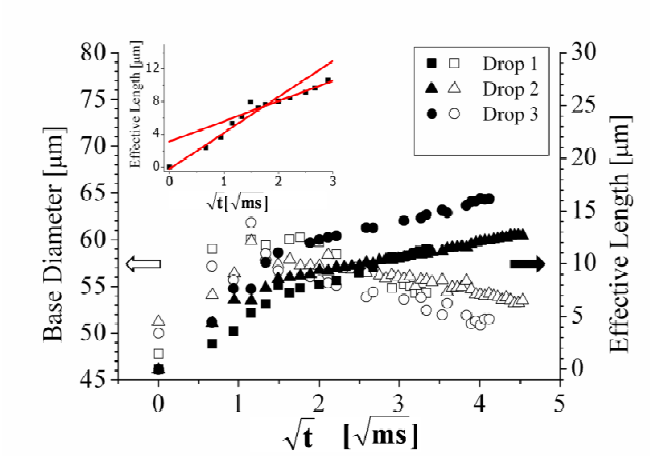

Figure 8. *Effective length (filled symbols) and base diameter (unfilled symbols) in micrometers (µm) vs. $\sqrt{t}$ ($\sqrt{ms}$) for three separate droplets impinged on matte coated paper. The inset shows trend lines marking the two regions displaying differences in linear coefficient of imbibition vs. $\sqrt{t}$.*

Discussion

The Initial droplet spreading period lasts about 1-2 ms on both the matte and the gloss coated papers (Figure 6 and Figure **8**), despite the significant differences in surface chemistry and roughness of the two (Table 1),

The linear curves in Figure 6 (gloss coated sample) suggest a Lucas-Washburn type of imbibition, with a possible contribution by diffusion processes arising from interactions between water and molecular moieties in the coating layer (e.g. binder, surfactants, slats). The reason behind the repeated divergence from the fitted linear curve, by the first - and to some extent - by the second point in each sequence remains to be explained.

The matte coated sample exhibits total drying times with a wider span relative to the ones observed on the gloss coated paper (30-100 ms relative to 10-13 ms, respectively), a consequence of the much larger structural and most probably chemical heterogeneities of the matte coated paper (Figure 5 and Figure 7). The trend of a decrease in the linear coefficient describing the rate of change in the effective length versus $\sqrt{t}$ (Figure 8) is particularly interesting. This can be rationalized by the Lucas-Washburn equation (Eq. 2) and taking into account the two distinct pore-populations mentioned above, as well as the layered structure of the coating. The Lucas –Washburn equation (Eq. 1) predicts a faster imbibition into large pores than into small ones with the same surface energy. In the matte coated sample the pore size difference between the two pore populations is two orders of magnitude. Consequently, in the initial few milliseconds most of the imbibition takes place in the large inter-aggregate pores, and hardly any in the small intra-aggregate pores. Later, a transition occur where imbibition is taking place mainly in the small intra-aggregate pores. Two scenarios can be the reason behind the latter transition: (1) The liquid front has reached the end of the silica gel aggregate layer and since most of the large pores are full imbibition takes place mostly inside the small, intra-aggregate pores. (2) While the liquid front advances, more and more small intra-aggregate pores are engaged in the imbibition. At a certain point all the liquid is consumed by imbibition taking place inside the small pores, thus

arresting the imbibition in the large pores. Both scenarios are suggested to result in the smaller linear coefficient describing the change in effective length vs. $\sqrt{t}$ (Figure 8). Interestingly enough, support for the second scenario can be found in the similarity between the effective length associated with the decrease in linear coefficient (6-11μm) and the thickness of the silica gel aggregate layer estimated by the aggregates size (about 1-15 μm, Figure 8) and the measured average peak-to-peak value (13 μm, Table 1).

Conclusions

In this work imbibition rates of pL-sized droplets on coated inkjet papers were measured and correlated with the coating layer structure. The ability to distinguish between the different imbibition events is enabled due to the combination of fast imaging and the use of small droplets. It was found that imbibition into the two discussed samples provides a linear relation between the change in effective length and the square root of time, which implies a Lucas-Washburn type of imbibition. In the case of the gloss coated paper, only one linear coefficient is observed, while in the case of the matte coated paper, two linear coefficients can be distinguished. We suggest that the first linear coefficient arises due to the dominating imbibition in the inter-aggregates pore population at short time scales, and the second linear coefficient arises due to imbibition in the smaller intra-aggregate pore population that dominates at longer time scales.

Acknowledgements

The grant from the Nils and Dorthi Troëdsson foundation for the combined Raman/AFM equipment, and from the Knut and Alice Wallenberg foundation for the XPS instrument are gratefully acknowledged. The authors thank Mikael Sundin (YKI) and Marie Ernstsson (YKI) for running the XPS and helping in interpretation, Birgit Brandner (YKI) for running the AFM, Norbert Heil (DataPhysics, Germany) for technical support of the OCA40 Instrument, and Kjell Jansson (Stockholm University) for helping with taking SEM images.

Appendix

Eq. 2 reads: $h_{eff} = c + \frac{V_0 - V(t)}{\pi R_d^2(t)}$ where h_{eff} is the effective length, $R_{\mathrm{d}}(t)$ the droplet base radius at time t, $V(t)$ the droplet volume at time t, and C and V_0 are two terms discussed below. h_{eff} is proportional to the difference between V_0 and $V(t)$, and inversely proportional to the droplet base area given by $\pi R_d^2(t)$. In the case where only one linear coefficient is observed (as on the gloss coated paper, Figure 6) C=0 and V_0 is the initial experimental volume at t=0 (captured in the first frame). When two linear coefficients are observed (matte coated paper, Figure 8), in the first stage corresponding to the first linear coefficient, C=0, and V_0 is the first experimentally observed volume, i.e. $V_0 = V(t=0)$. At a time t_2, the second stage starts, corresponding to the second linear coefficient. Here V_0 is the volume observed at the start of the second stage, i.e. $V_0 = V(t = t_2)$, and C is an offset term equals the effective length calculated at $t=t_2$ (start of the second stage) but with $V_0 = V(t = 0)$ (the volume captured at t=0, the start of the first stage). This procedure is justified by the assumption that the second stage is dominated by imbibition in the small intra-aggregate pores.

References

1. (a) Lucas, R., Ueber das Zeitgesetz des kapillaren Aufstiegs von Flüssigkeiten *Kolloid Zeitschrift* **1918,** *23*; (b) Washburn, E. W., The Dynamics of Capillary Flow *Physical review* **1921,** *17*.
2. (a) Fries, N.; Dreyer, M., The transition from inertial to viscous flow in capillary rise. *Journal of Colloid and Interface Science* **2008,** *327* (1), 125-128; (b) Zhmud, B. V.; Tiberg, F.; Hallstensson, K., Dynamics of capillary rise. *Journal of Colloid and Interface Science* **2000,** *228* (2), 263-269; (c) Quere, D., Inertial capillarity. *Europhysics Letters* **1997,** *39* (5), 533-538.
3. Oko, A.; Swerin, A.; Claesson, P., Imbibition and evaporation of water droplets on paper and solid impermeable substrates. 2010.
4. Daniel, R. C.; Berg, J. C., Spreading on and penetration into thin, permeable print media: Application to ink-jet printing. *Adv. Colloid Interface Sci.* **2006,** *123*, 439-469.

Author Biography

Asaf Oko received his BSc in Chemistry from the Hebrew University of Jerusalem, Israel (2008) and his MSc in material chemistry from Stockholm University, Sweden (2009). Since then he has been employed as a PhD student at YKI, Institute for surface chemistry (Stockholm, Sweden), in the Forest Products section.